Experimental research of different plasma cathodes for generation of high-current electron beams

G. Shafir,[1] M. Kreif,[1] J. Z. Gleizer,[1] S. Gleizer,[1] Ya. E. Krasik,[1] A. V. Gunin,[2] O. P. Kutenkov,[2] I. V. Pegel,[2,3] and V. V. Rostov[2]
[1]*Physics Department, Technion, Haifa 32000, Israel*
[2]*Institute of High Current Electronics, Siberian Branch, Russian Academy of Sciences, Tomsk 634055, Russia*
[3]*Tomsk Polytechnic University, Tomsk 634034, Russia*

(Received 11 September 2015; accepted 4 November 2015; published online 20 November 2015)

The results of experimental studies of different types of cathodes—carbon-epoxy rods, carbon-epoxy capillary, edged graphite, and metal-dielectric—under the application of high-voltage pulses with an amplitude of several hundreds of kV and pulse duration of several nanoseconds are presented. The best diode performance was achieved with the edged graphite and carbon-epoxy-based cathodes characterized by uniform and fast (<1 ns) formation of explosive emission plasma spots and quasi-constant diode impedance. This result was achieved for both annular cathodes in a strong magnetic field and planar cathodes of a similar diameter (~ 2 cm) with no external magnetic field. The cathodes based on carbon-epoxy rods and carbon-epoxy capillaries operating with an average current density up to 1 kA/cm^2 showed insignificant erosion along 10^6 pulses of the generator and the generated electron beam current showed excellent reproducibility in terms of the amplitude and waveform. © *2015 AIP Publishing LLC*. [http://dx.doi.org/10.1063/1.4935880]

I. INTRODUCTION

High-current electron beams of a few nanoseconds pulse duration are applied, mostly, in the generation of high power microwaves (HPM),[1,2] as well as in interdisciplinary studies employing nanosecond X-ray sources with planar diodes.[3] Among the different types of HPM devices, the Backward Wave Oscillator (BWO) has the lowest transition time, highest adaptivity to variation in electron beam parameters, and relatively high efficiency. Microwave generation efficiency in the K_a- and X-band of BWOs operating in quasi-stationary mode and supplied by high-voltage (HV) pulses ≤ 300 kV in amplitude and nanosecond timescale duration (≤ 4 ns) was shown to be in the range of (20%–30%).[1,4] The operation of the BWO is based on the interaction of the electrons of an annular beam during its transport in an external guiding magnetic field with synchronous minus-first harmonic of an axisymmetric wave in a corrugated circular waveguide (slow wave structure, SWS). An increase in the SWS length, with appropriate coupling profiling, allows the short-pulse super-radiance mode of BWO operation to be applied with fewer than 10 RF cycles. In this BWO operation mode, the conversion coefficient from electron beam power to microwave peak power can exceed 100%.[5] Moreover, it was shown[6] that decreasing the rise time of the acceleration voltage to sub-nanosecond timescale allows one to obtain HPM emission having oscillation phase stability. In recent research, in which a single HV generator producing at its output an amplitude of ~ 300 kV and a rise time in the sub-nanosecond timescale pulse was applied to several BWOs operating in parallel, phase matching of the generated high-power microwaves was achieved.[4,7,8]

Thus, the quality of the electron beam, namely, the amplitude of the current, energy spectrum, divergence, azimuthal uniformity, and reproducibility, can be considered crucial parameters for determining the BWO's efficiency and phase stability. The electron beam is generated from the boundary of the plasma formed at the surface of the cathode in magnetically insulated coaxial foilless diode.[9] Azimuthal uniformity in the density of this plasma determines the uniformity of the electron beam and the plasma axial expansion velocity dictates the matching between the impedances of the HV generator and diode, thus determining the energy spectrum and current of the electrons. Another important parameter is that a low-voltage threshold in the cathode plasma generation, resulting in a sub-nanosecond timescale time delay with respect to the beginning of the voltage pulse in the electron beam generation, is required.

During the last 30 years, different types of passive plasma cathode, i.e., when the plasma is generated by the voltage applied to the cathode, were investigated, namely, flashover[10] and explosive emission[11] plasma cathodes.

In the case of flashover plasma, different types of dielectric velvet and corduroy, low-conductive micron-scale carbon fibers, metal-ceramics, and multi-capillary-based cathodes were investigated (see Refs. 12–16 and references therein). It was found that the rise time of the electric field and its amplitude control the parameters of the plasma which is characterized by separate spots of plasma having a density and electron temperature $\leq 10^{16}$ cm^{-3} and ≤ 5 eV, respectively, and an expansion velocity of $\leq 2 \times 10^6$ cm/s. However, fast degradation of the emission properties of these cathodes was obtained when electron current densities >100 A/cm^2.

In the case of explosive emission cathodes, the rise time of the electric field also plays an important role in the formation of a larger number of explosion plasma spots. However, in this case the electric field enhancement at cathode micro-protrusions becomes a crucial issue in the formation of explosive emission spots. The plasma is characterized by

electron temperature of a few eV, expansion velocity of $\sim 2 \times 10^6$ cm/s, and drastic decrease in density with respect to the distance to the exploded micro-protrusions (at a distance of a few hundreds of μm, plasma density is $\leq 10^{17}$ cm^{-3}). In order to obtain a sub-nanosecond timescale in the formation of explosive plasma spots, one requires electric fields $\geq 10^7$ V/cm and a rise time $\geq 10^{15}$ V/(cm s). Explosive emission cathodes are used to generate electron beams with current densities ≥ 10 kA/cm^2. However, an increase of the repletion rate leads to a decrease in the number of plasma spots because of a smoothing of the cathode surface. To avoid this problem, a graphite cathode with edges specially sharpened down to tens of microns or carbon capillaries can be applied. The geometry of these cathodes provides a large enhancement of the electric field at the edges, and an additional increase in the electric field one obtains due to the existence of sub-μm scale micro-protrusions at the graphite surface. A large number of these micro-protrusions and their possible regeneration during the explosion serve as a good reason for applying this type of cathode in the generation of high-current density electron beams.

In the case of the BWO, one requires an appropriate cathode that provides the reproducible generation of azimuthally uniform annular electron beams with a current density of ≥ 1 kA/cm^2 and rise time $\leq 10^{-9}$ s. This generation should be delayed with respect to the beginning of the high-voltage pulse application $< 10^{-9}$ s. In addition, the cathode should have a long lifetime ($> 10^6$ pulses) and be compatible with operation at a high repetition rate (hundreds of Hz) without significant deterioration of the vacuum. In this paper, we describe the results of the research of several types of explosive emission cathodes for such a microwave source.

II. EXPERIMENTAL SETUP AND DIAGNOSTICS

The main part of the experiments was conducted using the experimental setup shown in Fig. 1. The electron beam was generated in a coaxial magnetically insulated foil-less electron diode.[9,17,18] The diode was supplied by an HV pulse generated by a semiconductor opening switch (SOS)-based generator[19] with internal impedance of 200 Ω. The generator produces pulses at a matched load of either 200 kV and 30 ns or 200 kV and 5 ns at Full Width Half Maximum (FWHM), depending on whether one or two magnetic compression stages are used. The output of the generator was connected to a cathode holder via an interface HV insulator. The cathode was placed in the tube, where a vacuum of ~13 mPa was maintained by a turbo-molecular pump. An anode drift tube 40 cm in length and 36 mm in inner diameter was placed

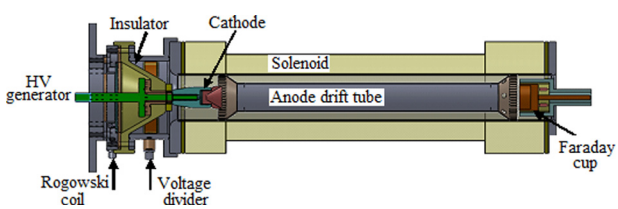

FIG. 1. Experimental setup.

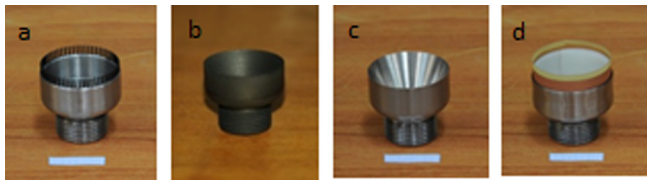

FIG. 2. Examples of cathodes. (a) Carbon-epoxy rod (0.7 mm diameter and 5 mm length) cathode; (b) graphite cathode; (c) edged stainless steel cathode; and (d) surface discharge cathode.

inside the stainless tube (inner diameter of 60 mm) at variable distances (5–20 mm) with respect to the cathode front edge surface. The stainless steel tube was located inside a solenoid producing a magnetic field of 2.5 T (axial non-uniformity ±1% along the distance of 70 cm) with a half period of 4.4 ms by the discharge of a preliminarily charged ($\leq$1.8 kV) high-energy density capacitor ($C = 4.15$ mF) using a vacuum triggered spark gap. The voltage and current waveforms were measured by a capacitive voltage divider and a self-integrating Rogowski coil, respectively. A low-inductance movable Faraday cup was used to measure the electron beam current at different distances of its transport inside the anode drift tube. The evolution of the space- and time-resolved electron plasma emission centers was observed using a fast-framing camera (Stanford Computer Optics model 4Quick05A) with frame duration of 3 ns. The electron beam pattern was characterized by placing a Mylar film inside the drift tube.

In this research, we studied different cathodes, all with an external diameter of 30 mm: *carbon fiber-based cathodes*, which include a carbon/epoxy capillary (Van Dijk Pultrusion Products) cathode and a carbon/epoxy rod cathode; *edged graphite cathodes* (thickness of 0.3 mm); *edged stainless steel cathodes* (thickness ≤ 20 μm); and *surface flashover-based cathode*. Examples of these cathodes are shown in Fig. 2.

Research of cathodes based on the same carbon-epoxy rods (0.7 mm diameter and 4 mm in length) and carbon-epoxy capillary (outer and inner diameters 0.7 mm and 0.2 mm, respectively, and 4 mm in length) as used in SOS generator experiments was also conducted in a planar diode supplied by HV pulses (280 kV) generated by a high-current (2 kA) and high-repetition rate (30–50 Hz) Sinus-150 generator.[20] By weighting the capillaries and rods it was shown that the specific density of both materials is the same. The rods (total number $N = 128$) were inserted into holes made in the cathode holder having a diameter of 28 mm, at a distance of 2 mm from each other (see Fig. 3). In order to avoid arcing

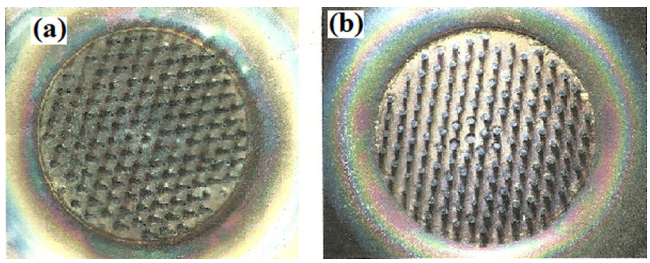

FIG. 3. External view of (a) carbon-epoxy capillary and (b) carbon-epoxy rod cathodes with screen electrode. Sinus-150 generator.

in the location of the contact rod (capillary)–cathode holder, these locations were carefully filled by solder. The cathode holder with the rods was inserted in a screen stainless steel electrode with a rounded edge having the same height as the rods. The design of the cathode was similar for the case of carbon-epoxy capillaries. The distance between the anode presenting the collector connected to the ground by low-inductance resistors, and the top of the rods was ~7 mm. The voltage was measured by a capacitive voltage divider placed in transformer oil at the output of the transmission line. The light emission from the plasma formed at the top of the rods (capillaries) was obtained from the front view using a digital camera PENTX-K200D operating with 1600 ISO sensitivity in the open shutter mode. In these experiments, the anode collector was replaced by a high transparency tungsten grid. The micro-structure of the rods (capillaries) was studied using scanning electron microscopy (SEM) with magnification up to 2000.

III. EXPERIMENTAL RESULTS AND DISCUSSION

A. Carbon/epoxy fiber based cathodes

Four types of carbon/epoxy fiber-based cathodes were investigated with an SOS-based generator: (1) 60 carbon/epoxy rods, 0.7 mm in diameter and 5 mm long; (2) 60 carbon/epoxy rods, 0.7 mm in diameter and 9 mm long; (3) 60 carbon/epoxy capillaries, 0.7 mm in external diameter, 0.3 mm in internal diameter, 5 mm long, and (4) 90 carbon/epoxy rods, 0.28 mm in diameter, 5 mm long. The rods (capillaries) were inserted in holes 0.71 mm or 0.31 mm in diameter which were made azimuthally uniform in the aluminum cathode holder and filled by silver-based glue. The glue that remained at the location of the contact rod (capillary) cathode holder was removed using acetone. The distance between the rods (capillaries) axes was 1.52 mm. All these types of carbon fiber cathodes, i.e., with different diameters and lengths, showed approximately the same results in experiments with HV pulse duration of either ~30 ns or ~5 ns at FWHM. Thus, here only the results of experiments with HV pulse duration of 30 ns are presented.

The typical results of the operation of the first type of cathode are presented in Fig. 4. One can see that the electron emission begins almost simultaneously (<1 ns) with the application of the HV pulse and the waveform of the emitted current follows that of the applied voltage. The average electric field was ~200 kV/cm and the total current was 1.5 kA, resulting in an average current from one rod of 25 A. The impedance of the diode, ~150 Ω, was quasi-constant within most parts of the HV pulse. This indicates a small axial plasma expansion during the applied pulse, as well as an almost constant number of plasma emission spots generated at the rod surface. The electron beam pattern shows that almost all the rods emit electrons rather uniformly and that there is strong electron magnetization. Namely, the typical pattern of a single micro-electron beam follows the form of the plasma spots formed at the rod surface and does not exceed 1 mm and 0.3 mm in diameter for carbon fiber rods with diameters of 0.7 mm and 0.28 mm, respectively. Let us note here that the cathode based on 0.28 mm diameter carbon fiber rods operated in a less robust form because of the low mechanical strength of the thin fibers, which caused misalignment of the rods with respect to the cathode holder.

Visible plasma light emission appears also at a time delay ≤1 ns with respect to the beginning of the HV pulse, showing azimuthal uniformity of separate plasma spots (3–5 plasma spots) generated at the front surface of each fiber. The brightness of the obtained individual plasma spots is almost equal, and the radial plasma light emission expansion was found to be negligibly small. This can be explained by a slow plasma expansion across the magnetic field. The Bohm diffusion coefficient for the plasma expansion in the transverse direction can be estimated as $D_\perp = ck_BT_e/16eB = 6.25 \cdot 10^6 T_e B^{-1} \approx 500\,\mathrm{cm}^2/\mathrm{s}$, where the electron temperature is assumed to be $T_e \approx 2\,\mathrm{eV}$, k_B is the Boltzmann constant, and c is the speed of light. Thus, the plasma expansion distance during 30 ns can be estimated as $\delta \approx \sqrt{D_\perp t} \leq 40\mu\mathrm{m}$. The smearing of light emission from plasma spots at the front surface of the fibers can be explained by the azimuthal drift of the plasma in $E_r \times B_\theta$ fields leading to overlapping of individual plasma spots.

In addition, side view images showed that the plasma formation occurs at the front surface of the carbon fiber. This indicates that an explosive emission phenomenon is responsible for the plasma formation. Here let us note that, assuming that the emitting surface of the plasma is around the cross-section of the fiber, one obtains that the average current density is ~6.5 kA/cm^2 and ~37 kA/cm^2 for fibers having a diameter of 0.7 mm and 0.28 mm diameter, respectively. Such a high-current density requires plasma

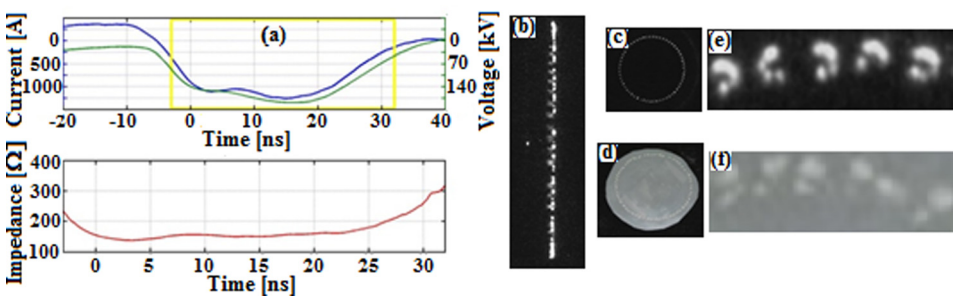

FIG. 4. SOS-based generator. Characterization of carbon fiber (rod diameter is 0.7 mm and length 5 mm) based cathode. (a) Current and voltage waveforms; (b) side-view; and (c) front-view images of light emission from the plasma spots; (d) zoomed front image of electron beam pattern; (e) light emission from the plasma formed at the front edge of the carbon-epoxy rods; and (f) electron beam pattern. Anode-cathode gap was 10 mm. Frame duration was 3 ns. Time delay of the frames (b), (c), and (e) with respect to the beginning of the voltage pulse was 10 ns.

density $\geq 2 \times 10^{15}\,cm^{-3}$ considering a plasma electron temperature of several eV. This explains the insignificant ($\sim$1 mm) visible axial expansion of the plasma, which agrees well with the quasi-constant diode impedance. Indeed, rough estimates showed that the plasma density even in individual plasma spots with a typical diameter of $\leq 10^{-2}$ cm will be $\sim 10^{18}\,cm^{-3}$; the plasma $\sim$1 mm expansion leads to a decrease in the density to $\sim 10^{15}\,cm^{-3}$. At this density, the plasma electron saturation and space-limited current densities becomes equal to each other, thus terminating plasma expansion.

Similar results were obtained for carbon-epoxy capillaries, i.e., several individual bright plasma spots at the top surface of each capillary, the absence of light emission from the side surface of the capillary and from the capillary inner volume, and negligible axial plasma light expansion. Thus, one can consider that also for carbon-epoxy capillaries the plasma is formed as a result of explosive emission processes.

In experiments with the Sinus-150 generator, the voltage amplitude and current was 277 ± 7 kV and 2.25 ± 0.25 kA, respectively, resulting in an average electric field of $\sim$400 kV/cm and diode impedance of $\sim$130 Ω. As in experiments with the SOS-based generator, the diode operation was comparable for carbon fiber and carbon-epoxy fiber cathodes. Namely, time integrated images (see Fig. 5) showed bright light emission spots at the front surface of fibers and capillaries with a typical size of 0.1–0.2 mm and the absence of light emission from the inner volume of the capillaries. An increase in the repetition rate from 1 Hz to 50 Hz did not show a difference in light emission from the plasma spots. The average number of plasma spots was estimated as $\sim$3 for each fiber, which gives a total number of spots of $\sim$384. Thus, an average current and current density from each plasma spot can be estimated as $\sim$6.25 A and $\sim$35 kA/cm^2, which is similar to those found in experiments with an SOS generator.

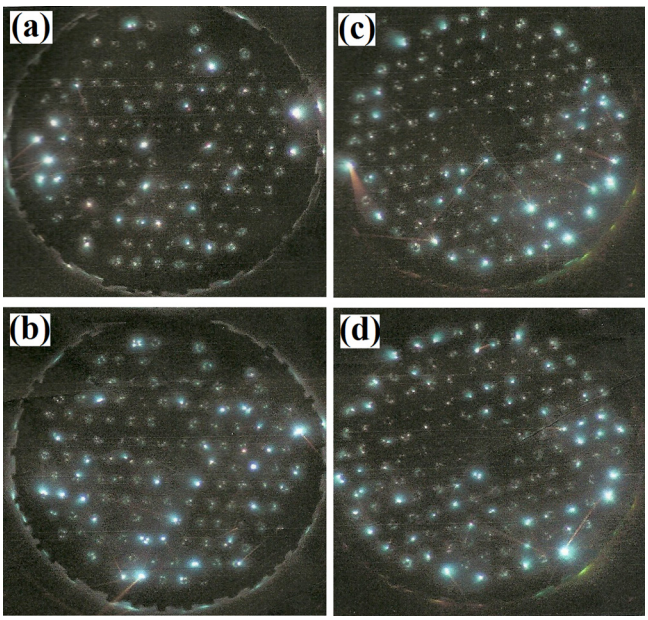

FIG. 5. Sinus-150 generator. Time integrated light emission of the plasma in the case of: (a) and (b) carbon fiber cathode; (c) and (d) carbon-epoxy capillary cathode. (a) and (c) and (b) and (d) repetition rate of the Sinus-150 generator operation is 1 Hz and 50 Hz, respectively.

These types of cathodes were tested for a lifetime, namely, 10^6 generator pulses produced with a repetition rate of 30 Hz. The results of these experiments do not show a difference in the voltage and current waveforms of the carbon fiber and carbon-epoxy capillary cathodes. In both cases, the amplitude of the diode current was 3.3 kA in the first pulses, decreased gradually to 2.5 kA within 10^3 pulses, and remained at this value during the following operation. In addition, in the first 10^3 pulses the time delay in the electron current appearance with respect to the beginning of the applied voltage was $<$0.5 ns. However, in the following pulses a typical peak in current with duration of $\sim$1 ns was obtained (see Fig. 6). This peak, having amplitude of $\sim$0.9 kA, corresponds to the charging current of the diode capacitance and it did not change during the 10^6-pulse lifetime test experiment. The larger amplitude of the diode current in the first 10^3 pulses is probably related to decontamination and degassing of the cathode surface.

Examples of the micro-structure of the carbon-epoxy capillary emitting surface after 10^6 pulses are shown in Fig. 7. One can see substantial erosion of the front surface and insignificant erosion of the external cylindrical surface of the capillary (see Fig. 7(b)). In addition, one can see destroyed edges of the capillary with a typical size of $\sim 10\,\mu$m, in particular, at its inner surface (see Fig. 7(d)) and melted fragments of larger dimensions. Qualitatively, the same microstructure of the front surface was obtained for rod emitting surfaces. The only difference obtained was in the form of the front surface. Namely, in the case of rods this surface remained flat and in that of capillaries it became like a cone. This can be related to slightly higher electrical conductivity through the lateral cylindrical surface of the capillary than through that of the rod. This results in a better electrical contact of this surface with the base of the cathode, a larger current flow in the surface layers of the capillary, and respectively, stronger material removal from the periphery at its edge. Nevertheless, the total erosion for rods and capillaries was almost the same and did not exceed 0.2 mm for 10^6 generator pulses.

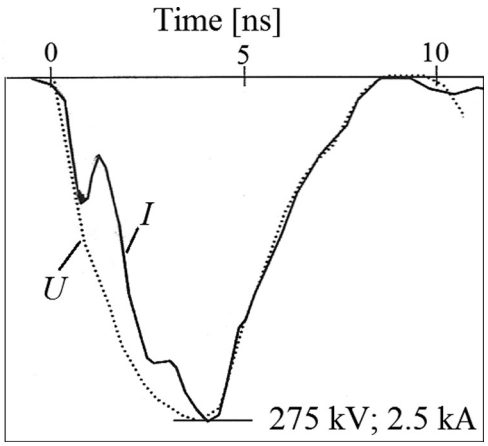

FIG. 6. Sinus-150 generator. Typical waveforms of the voltage U and current I after 10^5 pulses with carbon-epoxy capillary cathode.

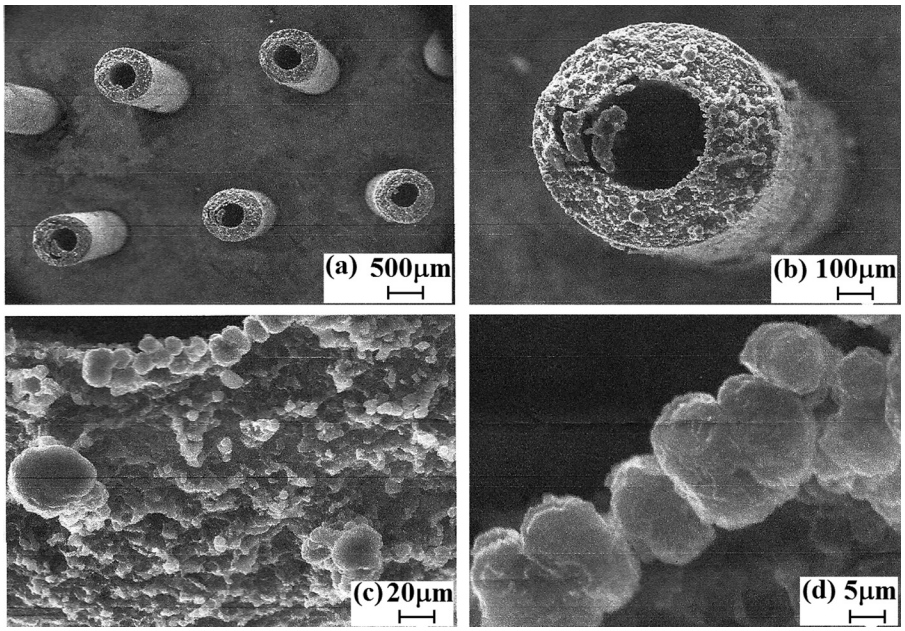

FIG. 7. SEM analysis of carbon-epoxy capillary emitting surface after 10^6 pulses of the Sinus-150 generator pulses.

Let us estimate the electron current emitted by the carbon fiber rod-based cathode considering the electron emission from the plasma spots generated simultaneously at the front surface of the fibers. The height h of the rods is significantly larger than the distance between the rods a (see Fig. 8). The form of the cathode plasma spots is semispherical with a typical radius R; the distance p between these hemispheres is smaller than the rod diameter d. Let us consider that the number of these plasma spots is 3 and that the average distance between these spots is $p \approx 0.4$ mm. In this case, within ~ 10 ns neighboring plasma spots will overlap each other because of the plasma expansion velocity $V_p \sim 2 \times 10^6$ cm/s. Thus, at time $t \ll 10$ ns one can consider that the electron emission from a single plasma spot is not screened by the space-charge of electrons emitted from the neighboring plasma spots. The amplitude of the electron current I (in CGS units) emitted by a single plasma spot can be estimated considering the space-charge-limited planar diode supplied by voltage with an amplitude U and with a cathode having a single plasma spot with a typical radius of R located at a distance D from the anode[21]

$$I = \beta\sqrt{\frac{e}{m}}\left(\frac{R}{D}U\right)^{3/2} = \beta\sqrt{\frac{e}{m}}(RE_1)^{3/2}. \quad (1)$$

Here, $\beta \approx 0.5$ is a typical dimensionless form-factor for a semispherical emitter and $E_1 = U/D$ is the average electric field. Let us note that Eq. (1) requires $D \gg R$ and $D/R \gg U$ [MV], which are satisfied by our experimental parameters. In the case of charge-limited electron emission, the electric field at the surface of the emitter is equal to zero, but at the typical distance R from the emitter the value of the electric field becomes approximately equal to E_1 due to the fast decrease in the electron space-charge density. This allows us to consider electron emission from the carbon fiber rod having a single semispherical emitter at its front surface and with an electric field E_1 in the vicinity of the rod for the case of the cathode with $N \gg 1$ rods. Here, we consider that the external electric field does not penetrate to the cathode holder, because $a \ll h$, which is realized in our experiments. In this case, the increase in the electric field in the vicinity of the rod is $\beta_1 = E_1/E_0 \approx (S_0/S_1)^{1/2}$, where S_0 and S_1 are the areas of the cathode holder and the total cross-sectional area of N rods, respectively. For our experimental parameters, $S_0 = 6\,\text{cm}^2$ and $S_1 \approx 0.5\,\text{cm}^2$, resulting in $\beta_1 \approx 3.5$ and $E_1 \approx 1.14$ MV for $E_0 \approx 400$ kV/cm.

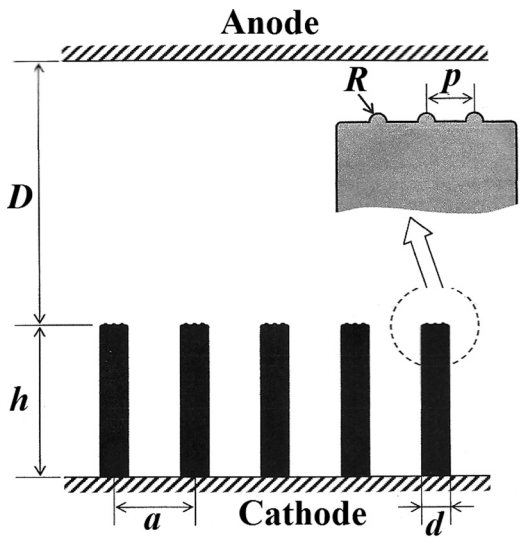

FIG. 8. Planar diode with carbon rod based cathode.

In the experiments, the maximum amplitude of the electron current was obtained at ~ 4 ns with respect to the beginning of the voltage pulse. Taking into account the ~ 1 ns time delay in the appearance of the plasma, one can consider the plasma expansion duration to be ~ 3 ns. This allows us to estimate the plasma spot radius as $R \approx 0.06$ mm, and respectively, the value of the current from a single fiber as $I \approx 12.2$ A, and the diode total electron current as ~ 4.7 kA, which is almost twice the experimentally measured current. This discrepancy can be related to different phenomena that

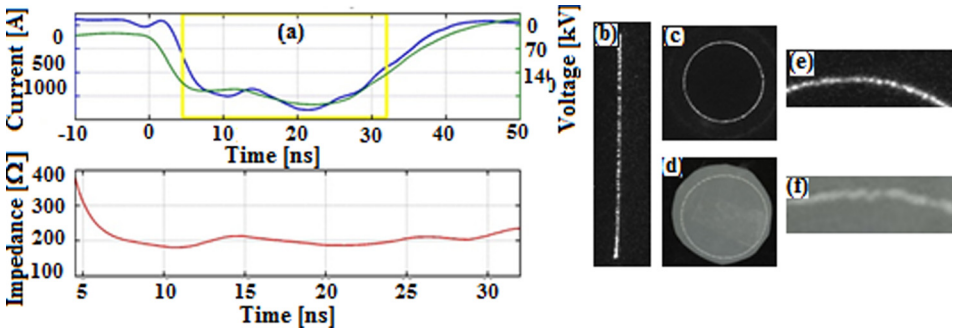

FIG. 9. Characterization of edged graphite cathode. SOS based generator. (a) Current and voltage waveforms; (b) side-view; and (c) front-view images of light emission from the plasma spots; (d) electron beam pattern; (e) zoomed front image of light emission from the plasma formed at the front edge of the graphite; and (f) electron beam pattern. Anode-cathode gap is of 10 mm. Frame duration of 3 ns. Time delay of the frames (b), (c), and (e) with respect to the beginning of the voltage pulse is 10 ns.

were not accounted for in this rough estimate, namely, non-simultaneous plasma spots generation, partial screening of the electric field of the single emitter by the space charge of electrons emitted by the neighboring emitter (see also Ref. 21), time-dependent velocity of the plasma expansion, etc.

Let us note that individual bright plasma spots generated at the top surface of the carbon-epoxy capillary, which indicates the explosive emission nature of the plasma formation, contradicts results obtained in earlier studies[22,23] of similar capillaries operating with an average electric field $\leq$150 kV and pulse duration of several hundreds of ns. This research showed that the plasma formation occurs inside the capillary. It is understood that additional experiments are required to understand this apparent contradiction.

B. Edged graphite cathode

The typical results of the operation of the edged graphite cathode supplied by HV pulses generated by an SOS-based generator are presented in Fig. 9. Both front and side views show very thin ($\sim$0.5 mm thick limited by space resolution of the framing camera) annular plasma light emission remaining uniform with rather high luminosity for tens of ns. This azimuthal light emission is characterized by brighter spots, the number of which exceeds significantly that of bright emission spots obtained in the case of the carbon-epoxy rod or carbon-epoxy capillary cathode operations. Thus, this cathode showed an azimuthal uniformity of plasma emission centers that is better than that of the carbon-epoxy rod or carbon-epoxy capillary cathodes., These plasma emission centers are ignited almost simultaneously within $<$1 ns with respect to the beginning of the voltage pulse. The smeared light emission between the plasma spots can be explained by the plasma azimuthal drift in $E_r \times B_z$ fields. For this type of the cathode also, the diode impedance remains almost constant at $\sim$200 Ω throughout the HV pulse. Thus, similar to the case of carbon-epoxy rod or carbon-epoxy capillary cathodes, axial plasma expansion leads to a drastic decrease in the plasma density versus the distance from the cathode, and at a distance of $\sim$1 mm from the cathode the plasma saturation electron current density becomes equal to the space-charge limited current density. The measured width of the electron beam pattern is $\leq$0.3 mm, resulting in an average electron beam current density of $\sim$350 A/cm^2.

C. Edged stainless steel cathode

The typical results of the edged stainless steel cathode operation with SOS generator are shown in Fig. 10. One can see that, in spite of the cathode edge thickness $\leq$20 μm, which should lead to significant electric field enhancement at this location, there is a $\sim$5 ns time delay in appearance of the electron emission, which agrees with the same time delay in the appearance of visible light emission from the plasma spots formed at the cathode edges. One can also see that there is azimuthal non-uniformity in the location of these plasma spots. Respectively, the intensity of the pattern of the electron beam is non-azimuthally symmetrical. The number of plasma spots increases in time and only at time $>$30 ns of

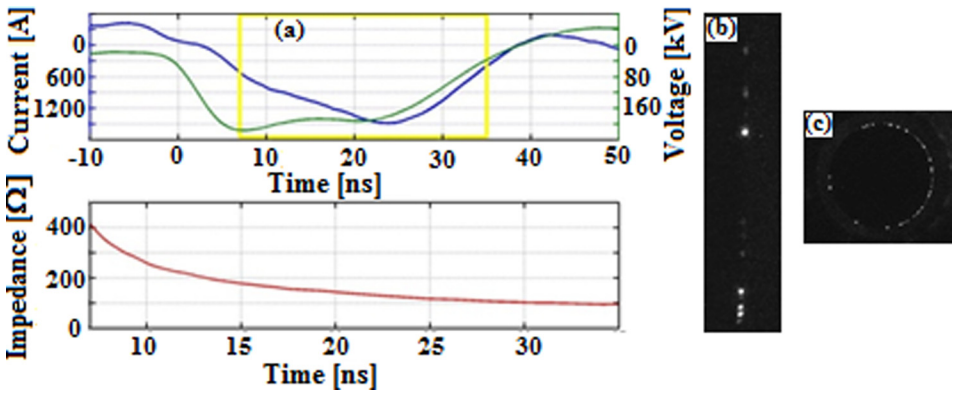

FIG. 10. Characterization of stainless steel cathode. SOS based generator. (a) Current and voltage waveforms; (b) side-view; and (c) front-view images of light emission from the plasma spots. Anode-cathode gap of 9.5 mm. Frame duration of 3 ns. Time delay of frames (b) and (c) with respect to the beginning of the voltage pulse is 15 ns.

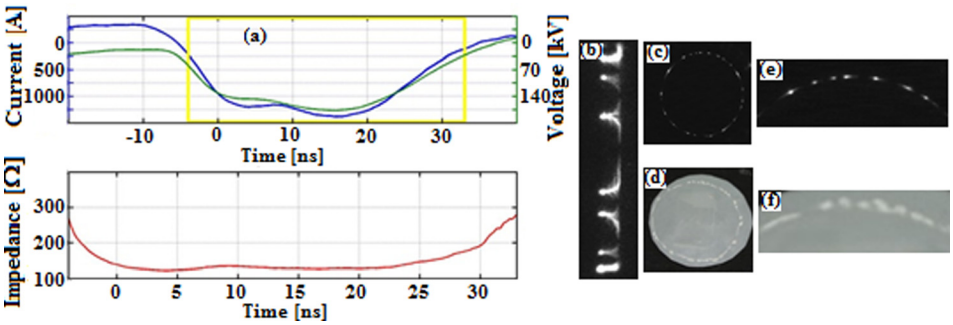

FIG. 11. Characterization of surface discharge cathode. SOS based generator. (a) Current and voltage waveforms; (b) side-view; and (c) front-view images of light emission from the plasma spots; (d) electron beam pattern; (e) zoomed front image of light emission from the plasma formed at the front edge of the graphite; and (f) electron beam pattern. Anode-cathode gap of 9.5 mm. Frame duration of 3 ns. Time delay of the frames (b), (c), and (e) with respect to the beginning of the voltage pulse is 15 ns.

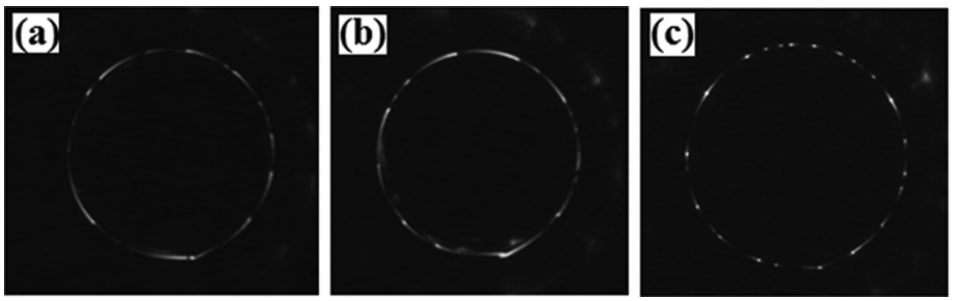

FIG. 12. SOS based generator. Operation of surface discharge cathode in different magnetic fields: (a) magnetic field in the +z direction; (b) magnetic field in the −z direction; (c) without magnetic field. Frame duration of 3 ns. Time delay of the frames (b), (c), and (e) with respect to the beginning of the voltage pulse is 20 ns.

the HV pulse does one obtain plasma light emission from almost the entire cathode edge. The amplitude of the diode current reaches 1500 A but with a time delay of 20 ns with respect to the peak voltage, resulting in a gradual decrease of the diode impedance. Here, let us note that with a 5 ns FWHM duration HV pulse, the cathode plasma spots ignition was faster (∼1 ns), but the number of plasma spots was smaller in spite of the larger dE/dt of the applied electric field. These results suggest that only a few explosive emission plasma spots appear as the voltage pulse is applied. Since the current is space-charge limited and the total emission surface is small, the current is relatively low at the beginning of the pulse. However, the density of the current extracted from each plasma spot is significantly larger than for the carbon-based cathodes. The latter allows one to consider a significantly larger density and temperature of the spot plasma. Later, due to the appearance of new explosive emission plasma spots and plasma expansion mainly along the magnetic field lines, the space-charge limited current rises rapidly. This plasma expansion causes a diode impedance mismatch and fast decrease in the voltage. Using a planar diode for side-view observation of the cathode plasma spots without magnetic field, the axial plasma expansion velocity was estimated as $\sim 4 \times 10^6$ cm/s. Similar experiments, with all the carbon-based cathodes, showed negligible plasma expansion that qualitatively agrees with a lower density of the plasma formed at the surface of these cathodes.

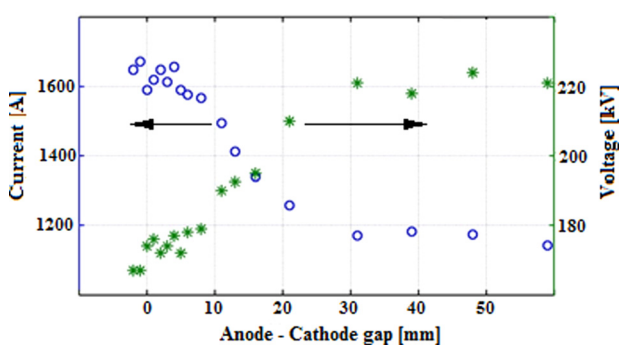

FIG. 13. Diode current and diode voltage versus anode-cathode gap. SOS based generator.

D. Surface flashover cathode

The surface flashover cathode was made of fiber-glass plate (∼100 μm thick) with a glued copper film ∼50 μm thick. From the anode side, 3 mm of the copper film was removed at the edge of the plate. This plate was installed in the cathode holder forming a ring type cathode. The typical results of this cathode operation with the SOS generator are presented in Figs. 11 and 12. One can see that the voltage and current waveforms are similar to those obtained for carbon fiber rod- and capillary-based cathodes (almost simultaneous appearance of the electron emission, quasi-constant diode impedance, etc.). However, this type of cathode showed different features of the plasma formation. When the HV pulse is applied, the discharges are ignited at triple junctions (metal-insulator-vacuum junctions) and expand over the insulator surface, smearing in the azimuthal direction. We note that this process occurs very fast, within ∼1 ns. This allows electron acceleration from almost the entire surface of the insulator, resulting in a high-current annular electron beam being generated. However, the beam is not uniform in the azimuthal direction, as higher electron density is observed at the angles of the discharge initiation. The flashover plasma experiences an $E_r \times B_z$ azimuthal drift, which was confirmed by changing the direction of the magnetic field and comparing the plasma flow with that produced

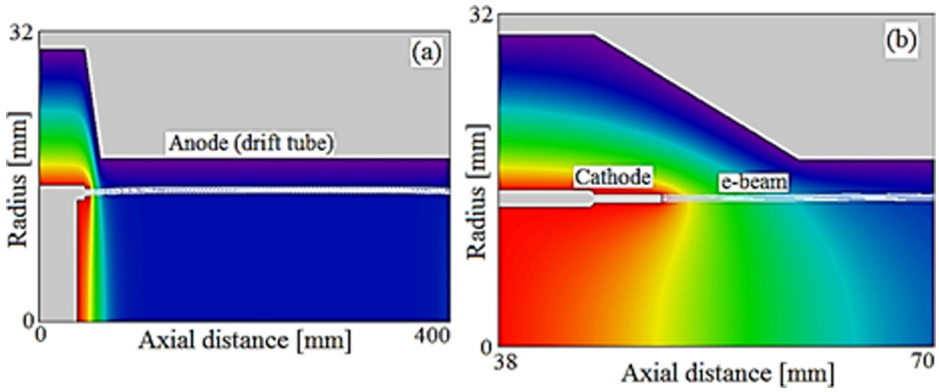

FIG. 14. Ray tracing simulation of the electron beam in the foil-less diode and drift tube. (a) Entire system (axial axis is not scaled). (b) Zoom of cathode-anode area. The electron beam is shown on the background of the calculated potential, from −200 kV (red) to 0 (purple).

with a zero magnetic field, as shown in Fig. 12. One can see that the direction of the magnetic field is changed, the azimuthal plasma flow direction is inversed; without a magnetic field, it is dramatically reduced with no favored direction.

E. Electron beam current at different cathode-anode gaps

In order to test the Volt-Ampere parameters of the magnetically insulated foil-less diode operated with an SOS generator, the diode voltage and current were measured for different anode-cathode distances. These measurements were performed with the cathode based on carbon fibers, 0.7 mm diameter and 5 mm long. The dependences of the diode current and voltage at the peak current time versus the anode-cathode gap are shown in Fig. 13. One can see that a ∼200 Ω impedance of the diode is reached at an anode-cathode distance of ≥30 mm. When the anode-cathode gap is ≥30 mm, a plateau in the diode current/voltage is reached. This matches the condition where the anode-cathode gap is larger than the drift tube radius (see Fig. 1) and the amplitude of the generated electron current amplitude is determined by the radius of the external tube, which serves as the actual anode.

In order to derive an exact solution of the space-charged-limited flow in the foil-less magnetically insulated diode, ray-tracing simulation was conducted.[24] An annular azimuthally uniform emission cathode (at a constant potential of −200 kV) 30 mm in diameter and 0.7 mm in thickness was placed 50 mm inside the solenoid with a constant magnetic field of 2.5 T. The anode, with an inner diameter of 36 mm, was placed at different distances from the cathode. A typical electric potential distribution and electron beam tracks for a 10 mm anode–cathode gap are shown in Fig. 14. The total emitted current for this configuration is 1.8 kA.

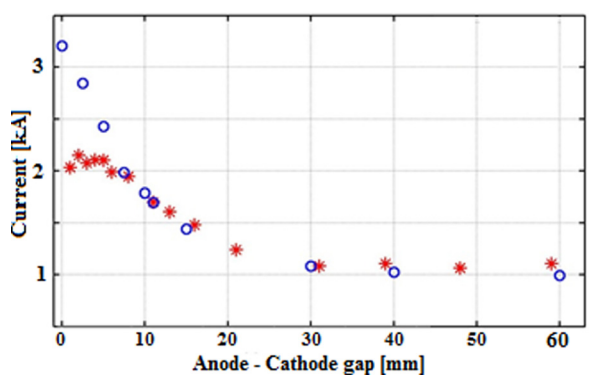

FIG. 15. Normalized measured current and simulated current versus anode-cathode gap. Stars—diode current and circles—simulated diode current.

Here, let us note that the experimentally measured electron beam is composed of 60 separate beams, each with a diameter of ∼0.7 mm resulting in ∼40% of the simulated current where the area of simulated perfect annulus is 62.7 mm^2. Thus, the measured electron beam current was normalized by this value, allowing a comparison with the simulation results; see Fig. 15 showing a good match with the measured current.

IV. SUMMARY

In this research, we investigated the operation of several different cathodes, operated in a foil-less magnetically insulated diode and planar diode supplied by several hundreds of kV pulses with a duration 5–30 ns. It was found that the best diode performance was achieved with the edged graphite and carbon fiber composite-based cathodes. Namely, the cathode ignition, i.e., plasma formation, was azimuthally uniform and fast (<1 ns), and the diode impedance was almost constant throughout the applied HV pulse duration. In terms of handling, the graphite cathode is better than the carbon fiber composite cathode and easier to manufacture and use. All the carbon fiber rod- and capillary-based cathodes operated similarly, with plasma generation only at the rod/capillary edges. This indicates the generation of explosive emission plasma with a density that decreases drastically versus the distance from the cathode, thus allowing one to obtain quasi-constant impedance of the diode operation. A negligible small erosion of the carbon-epoxy rod- and capillary-based cathodes was obtained in lifetime test experiments for 10^6 pulses of the Sinus-150 generator with sufficiently good reproducibility in current and voltage waveforms. Thus, the results obtained suggest that these cathodes are good candidates for the generation of high-current electron beams for backward-wave oscillator microwave sources operating with nanosecond timescale duration pulses.

ACKNOWLEDGMENTS

The authors are grateful to A. Fisher and A. Shlapakovski for fruitful discussions and to N. Gruzinski and E. Flyatt for perfect technical assistance. This work was supported in part by the PAZY Grant No. 2020960.

[1]V. P. Gubanov, S. D. Korovin, I. V. Pegel, A. M. Roitman, V. V. Rostov, and A. S. Stepchenko, IEEE Trans. Plasma Sci. **25**, 258 (1997).
[2]G. A. Mesyats, S. D. Korovin, V. V. Rostov, V. G. Shpak, and M. I. Yalandin, "The RADAN series of compact pulsed power generators and their applications," Proc. IEEE **92**, 1166 (2004).
[3]K. V. Afanas'ev, M. I. Vagner, O. P. Kutenkov, I. V. Pegel, G. A. Pribytkov, V. V. Rostov, and V. P. Tarakanov, Russ. Phys. J. **55**, 772 (2012).
[4]A. A. El'chaninov, A. I. Klimov, I. V. Romanchenko, V. V. Rostov, M. S. Pedos, S. N. Rukin, K. A. Sharypov, V. G. Shpak, S. A. Shunailov, M. R. Ul'maskulov, and M. I. Yalandin, Tech. Phys. Lett. **39**, 910 (2013).
[5]A. A. El'chaninov, S. D. Korovin, V. V. Rostov, I. V. Pegel, G. A. Mesyats, M. I. Yalandin, and N. S. Ginzburg, JETP Lett. **77**, 266 (2003).
[6]K. V. Afanas'ev, N. M. Bykov, V. P. Gubanov, A. A. El'chaninov, A. I. Klimov, S. D. Korovin, V. V. Rostov, and A. S. Stepchenko, Tech. Phys. Lett. **32**, 925 (2006).
[7]V. V. Rostov, A. A. El'chaninov, I. V. Romanchenko, and M. I. Yalandin, Appl. Phys. Lett. **100**, 224102 (2012).
[8]K. A. Sharypov, A. A. El'chaninov, G. A. Mesyats, M. S. Pedos, I. V. Romanchenko, V. V. Rostov, S. N. Rukin, V. G. Shpak, S. A. Shunailov, M. R. Ul'masculov, and M. I. Yalandin, Appl. Phys. Lett. **103**, 134103 (2013).
[9]R. B. Miller, *An Introduction to the Physics of Intense Charged Particle Beams* (Plenum Press, New York, 1982).
[10]R. B. Miller, "Mechanism of explosive electron emission for dielectric fiber (velvet) cathodes," J. Appl. Phys. **84**, 3880 (1998).
[11]G. A. Mesyats, *Explosive Electron Emission* (URO, Ekaterinburg, 1998).
[12]Ya. E. Krasik, A. Dunaevsky, A. Krokhmal, J. Felsteiner, A. V. Gunin, I. V. Pegel, and S. D. Korovin, J. Appl. Phys. **89**, 2379 (2001).
[13]Ya. E. Krasik, A. Dunaevsky, J. Felsteiner, J. Z. Gleizer, Yu. A. Kotov, S. Yu. Sokovnin, and M. E. Balezin, J. Appl. Phys. **91**, 9385 (2002).
[14]Ya. E. Krasik, J. Z. Gleizer, D. Yarmolich, A. Krokhmal, V. Ts. Gurovich, E. Efimov, J. Felsteiner, V. Bernshtam, and Yu. M. Saveliev, J. Appl. Phys. **98**, 093308 (2005).
[15]Ya. E. Krasik, A. Dunaevsky, and J. Felsteiner, Eur. Phys. J. D **15**, 345 (2001).
[16]J. Z. Gleizer, Y. Hadas, D. Yarmolich, J. Felsteiner, and Ya. E. Krasik, Appl. Phys. Lett. **90**, 181501 (2007).
[17]J. Chen and R. V. Lovelace, Phys. Fluids **21**, 1623 (1978).
[18]E. Ott, T. M. Antonsen, and R. V. Lovelace, Phys. Fluids **20**, 1180 (1977).
[19]S. N. Rukin, Instrum. Exp. Tech. **4**, 439 (1999).
[20]V. P. Gubanov, A. V. Gunin, S. D. Korovin, and A. S. Stepchenko, Prib. Tekh. Eksp. (Russ.) **1**, 73 (2002).
[21]S. Ya. Belomytsev, S. D. Korovin, and I. V. Pegel, IEEE Trans. Plasma Sci. **27**, 1572 (1999).
[22]T. Queller, J. Z. Gleizer, Y. E. Krasik, V. A. Bernshtam, and U. Dai, IEEE Trans. Plasma Sci. **42**, 1224 (2014).
[23]E. E. Rocha, P. M. Kelly, J. M. Parson, C. F. Lynn, J. C. Dickens, A. A. Neuber, J. J. Mankowski, T. Queller, J. Gleizer, and Ya. E. Krasik, IEEE Trans. Plasma Sci. **43**, 2670 (2015).
[24]S. Humphries, See http://www.fieldp.com for FIELD PRECISION Tricomp group of codes developed.